Dynamics in Host–Guest Complexes of Molecular Tweezers and Clips

Matthias Lobert, Heinz Bandmann, Ulrich Burkert, Uta P. Büchele, Viola Podsadlowski, and Frank-Gerrit Klärner*[a]

Abstract: The dynamics in the host–guest complexes of the molecular tweezers **1a,b** and clips **2a,b** with 1,2,4,5-tetracyanobenzene (TCNB, **3**) and tropylium tetrafluoroborate (**4**) as guest molecules were analyzed by temperature-dependent ^1H NMR spectroscopy. The TCNB complexes of tweezers **1a,b** were found to be particularly stable (dissociation barrier: $\Delta G^{\ddagger} = 16.8$ and 15.7 kcal mol^{-1}, respectively), more stable than the TCNB complexes of clips **2a,b** and the tropylium complex of tweezer **1b** (dissociation barrier: $\Delta G^{\ddagger} = 12.4$, 11.2, and 12.3 kcal mol^{-1}, respectively). A detailed analysis of the kinetic and thermodynamic data (especially the negative entropies of activation found for complex dissociation) suggests that in the transition state of dissociation the guest molecule is still clipped between the aromatic tips of the host molecule. The ^1H NMR analysis of the TCNB complexes **3@1b** and **3@2a** at low temperatures ($T < -80\,°C$) showed that **3** undergoes fast rotation inside the cavity of tweezer **1b** or clip **2a** (rotational barrier: $\Delta G^{\ddagger} = 11.7$ and 8.3 kcal mol^{-1}, respectively). This rotation of a guest molecule inside the host cavity can be considered to be the dynamic equilibration of noncovalent conformers. In the case of clip complex **3@2a** the association and rotational barriers are smaller by $\Delta\Delta G^{\ddagger} = 3–4$ kcal mol^{-1} than those in tweezer complexes **3@1a,b**. This can be explained by the more open topology of the trimethylene-bridged clips compared to the tetramethylene-bridged tweezers.

Keywords: host–guest systems · kinetics · molecular recognition · NMR spectroscopy · supramolecular chemistry

Finally, the bromo substituents in the newly prepared clip **2b** have a substantial effect on the kinetics and thermodynamics of complex formation. Clip **2b** forms weaker complexes with (TCNB, **3**) and tetracyanoquinodimethane (TCNQ, **12**) and a more stable complex with 2,4,7-trinitrofluoren-9-ylidene (TNF, **13**) than the parent clip **2a**. These results can be explained by a less negative electrostatic potential surface (EPS) inside the cavity and a larger van der Waals contact surface of **2b** compared to **2a**. In the case of the highly electron-deficient guest molecules TCNB and TCNQ the attractive electrostatic interaction is predominant and hence responsible for the thermodynamic complex stability, whereas in the case of TNF with its extended π system, dispersion forces are more important for host–guest binding.

Introduction

Supramolecular chemistry deals with the development and function of complex chemical systems.[1–3] They are formed by association from smaller molecular components held together by noncovalent bonds in well-defined structures under thermodynamic control. Dynamic processes determine the kinetic stabilities and hence the properties of supramolecular associates.[4] Systems are known which are stable at room temperature, for example, the hemicarceplexes of Cram et al., which consist of hemicarcerand host molecules and small guest molecules.[5,6] Exit and entry of the guest molecule proceed only at higher temperature with a substantial activation barrier resulting from opening and closing of a gate by conformational distortion of the host geometry, which is required for guest movement in- and outside the host cavity.[7,8] Other examples of kinetically highly stable supramolecules are the catenanes[9] and rotaxanes,[10–12] in which two or more rings or a molecular wheel and a molecular axis are mechanically interlocked. In these systems the intramolecular dynamics (in catenanes, movement of the rings relative to each other, and in the rotax-

[a] Dr. M. Lobert, Dipl.-Ing. H. Bandmann, Dr. U. Burkert,
Dr. U. P. Büchele, Dr. V. Podsadlowski, Prof. Dr. F.-G. Klärner
Institut für Organische Chemie
Universität Duisburg-Essen
45117 Essen (Germany)
Fax: (+49)201-183-4252
E-mail: frank.klaerner@uni-essen.de

Supporting information for this article is available on the WWW under http://www.chemeurj.org/ or from the author.

anes, "shuttling" of the wheel along the molecular axis)[13,14] are of considerable interest, for example, in connection with the construction of molecular devices.[15] However, most supramolecules (host–guest complexes,[16–20] molecular capsules,[21,22] rosettes,[23,24] helicates,[25] etc.) result from formation of noncovalent bonds, which usually occurs in diffusion-controlled processes. Thus, these associates are kinetically not very stable and dissociation proceeds rapidly. Here we report on the dynamics in host–guest complexes of molecular tweezers **1a,b** and clips **2a,b**.

We recently described the syntheses and some supramolecular properties of the new host molecules **1a,b**[26–29] and **2a**,[30] named molecular tweezers and clips.[31] The size
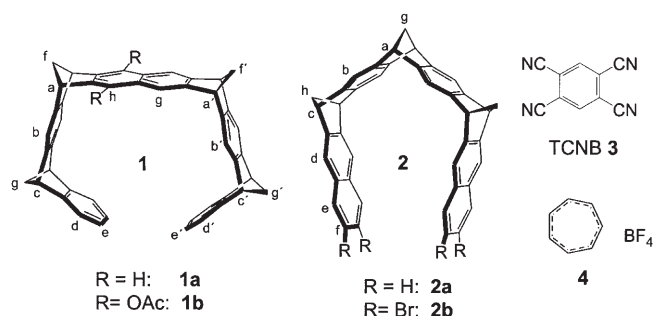
and shape of their cavities depends on the number of methylene bridges and on the size of the aromatic spacer units (benzene or naphthalene). These host molecules selectively bind electron-deficient aromatic neutral and cationic guests inside their cavity by multiple attractive noncovalent CH–π and π–π interactions. Electron-rich arenes or anions are not bound by these hosts within the limits of experimental detection. This high selectivity for electron-deficient guest molecules was explained by the markedly negative electrostatic surfaces (EPSs) calculated for the concave faces of **1a,b** and **2a** by quantum chemical methods.[32,33] When analogous calculations were performed for electron-deficient guest molecules binding to **1a,b** and **2a**, the complementary nature of their positive EPSs became evident, and this suggests that host–guest binding in these complexes is predominantly electrostatic in nature. This report focuses on the dynamics of host–guest binding, the dissociation/association process, and the mobility of the guest molecule inside the tweezer or clip cavity. Furthermore, we describe the synthesis of hitherto-unknown tetrabromo-substituted clip **2b** and the kinetics and thermodynamics of its complex formation with various electron-deficient guest molecules. One aim of this study is to find out whether the kinetic complex stability correlates with the topology of the tweezer or clip.

Results and Discussion

The parent naphthalene-spaced molecular tweezer **1a** forms a stable, bright yellow complex with 1,2,4,5-tetracyanoben-

zene (TCNB, **3**).[27] In this case complex dissociation and association are slow processes with respect to the NMR timescale, so that at room temperature in the ¹H NMR spectrum of a 2:1 mixture of **1a** and **3** separate signals of empty and complexed **1a** are observed, which coalesce at 81 °C. From the analysis of the temperature-dependent line shapes of
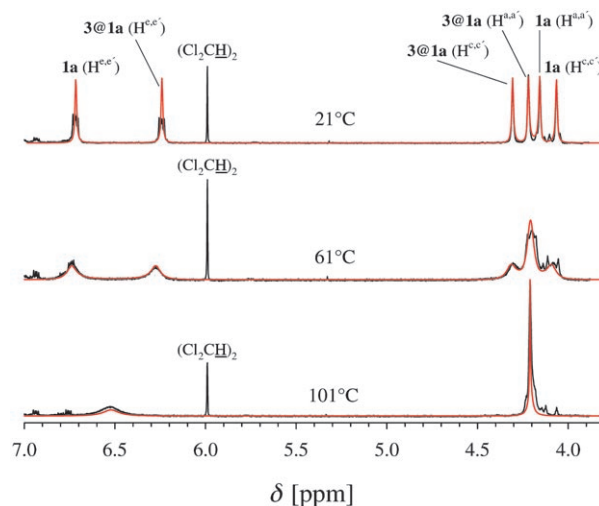

Figure 1. ¹H NMR spectra (300 MHz, (CDCl₂)₂) of tweezer **1a** and TCNB **3** ([**1a**]₀=0.02 M, [**3**]₀=0.01 M) at different temperatures. The superimposed red-line fit to the peaks results from line-shape analysis.

these signals (Figure 1), the specific rate constants, and hence the activation parameters (Gibbs enthalpy ΔG^{+}, enthalpy ΔH^{+}, and entropy ΔS^{+} of activation) of the mutual exchange of the TCNB guest molecule between complex **3@1a** and empty tweezer **1a** could be determined (Table 1a, Figure 2a).

Table 1. Temperature dependence of the specific rate constants of exchange of guest between the host–guest complex and empty host, determined from line-shape of the exchanging-host signals in the ¹H NMR spectra of a 2:1 mixture of host and guest: a) tweezer **1a** and TCNB (**3**) (300 MHz, (CDCl₂)₂); b) clip **2a** and TCNB (**3**) (500 MHz, [D₈]toluene); c) tweezer (**1b**) and tropylium tetrafluoroborate (**4**) (500 MHz, CDCl₃/CD₃OD 1/1); d) clip **2b** and TCNB (**3**) (500 MHz, [D₈]toluene).

a		b		c		d	
T [°C]	k [s⁻¹]	T [°C]	k [s⁻¹]	T [°C]	k [s⁻¹]	T [°C]	k [s⁻¹]
21	7	−40	23	−50	20	−80	11
41	12	−25	65	−5	580	−70	25
61	60	−18	132	10	1600	−60	75
81	190	−15	168	25	5550	−20	1087
101	1100	−13	206	55	15000	25	5633
		5	710				

Similar results were obtained for complex formation between diacetoxy-substituted tweezer **1b** and TCNB (**3**). In the ¹H NMR spectrum of 2:1 mixture of **1b** and **3** separate signals at δ=5.86 and 5.51 ppm can be assigned to the pro-
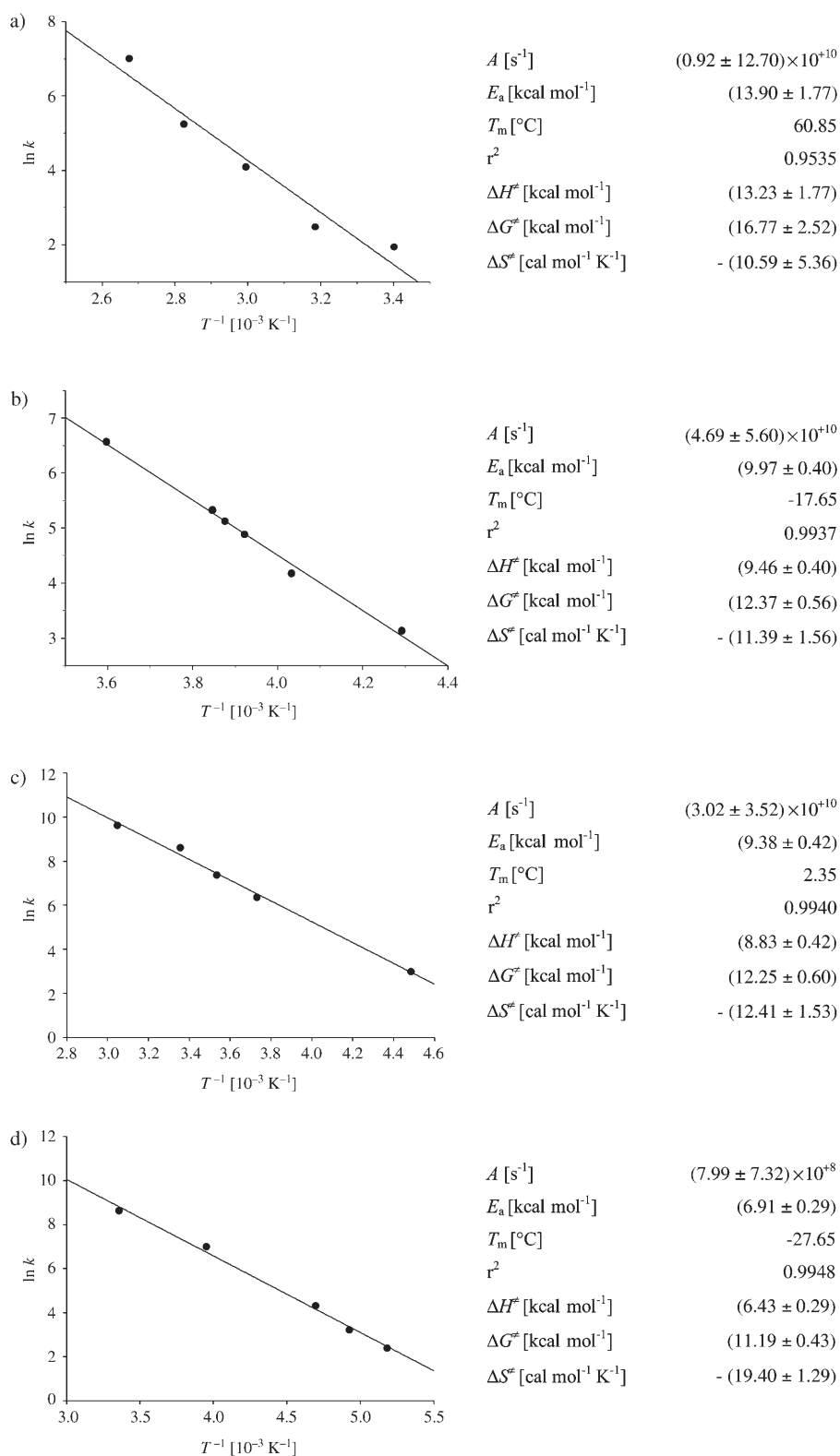
a)

A [s^{-1}]	$(0.92 \pm 12.70) \times 10^{+10}$
E_a [kcal mol^{-1}]	(13.90 ± 1.77)
T_m [°C]	60.85
r^2	0.9535
$\Delta H^{\neq}$ [kcal mol^{-1}]	(13.23 ± 1.77)
$\Delta G^{\neq}$ [kcal mol^{-1}]	(16.77 ± 2.52)
$\Delta S^{\neq}$ [cal mol^{-1} K^{-1}]	$- (10.59 \pm 5.36)$

b)

A [s^{-1}]	$(4.69 \pm 5.60) \times 10^{+10}$
E_a [kcal mol^{-1}]	(9.97 ± 0.40)
T_m [°C]	-17.65
r^2	0.9937
$\Delta H^{\neq}$ [kcal mol^{-1}]	(9.46 ± 0.40)
$\Delta G^{\neq}$ [kcal mol^{-1}]	(12.37 ± 0.56)
$\Delta S^{\neq}$ [cal mol^{-1} K^{-1}]	$- (11.39 \pm 1.56)$

c)

A [s^{-1}]	$(3.02 \pm 3.52) \times 10^{+10}$
E_a [kcal mol^{-1}]	(9.38 ± 0.42)
T_m [°C]	2.35
r^2	0.9940
$\Delta H^{\neq}$ [kcal mol^{-1}]	(8.83 ± 0.42)
$\Delta G^{\neq}$ [kcal mol^{-1}]	(12.25 ± 0.60)
$\Delta S^{\neq}$ [cal mol^{-1} K^{-1}]	$- (12.41 \pm 1.53)$

d)

A [s^{-1}]	$(7.99 \pm 7.32) \times 10^{+8}$
E_a [kcal mol^{-1}]	(6.91 ± 0.29)
T_m [°C]	-27.65
r^2	0.9948
$\Delta H^{\neq}$ [kcal mol^{-1}]	(6.43 ± 0.29)
$\Delta G^{\neq}$ [kcal mol^{-1}]	(11.19 ± 0.43)
$\Delta S^{\neq}$ [cal mol^{-1} K^{-1}]	$- (19.40 \pm 1.29)$

Figure 2. Arrhenius plots ($\ln k$ vs T^{-1} [K^{-1}]) and activation parameters (enthalpy $\Delta H^{\neq}$, entropy $\Delta S^{\neq}$, and Gibbs enthalpy $\Delta G^{\neq}$ of activation) resulting from the temperature dependence of the specific rate constants k listed in Table 1 for complex formation between a) **1a** and **3**; b) **2a** and **3**, c) **1b** and **4**, and d) **2b** and **3**.

change is again slow with respect to the NMR timescale. Also in this case an increase in temperature leads to specific broadening and finally to coalescence of the exchanging signals. Because of partial overlap of the exchanging signals we could not perform a complete line-shape analysis and could only estimate the rate constant ($k_c \approx 313$ s^{-1}) and Gibbs activation enthalpy ($\Delta G \approx 15.7$ kcal mol^{-1}) at 60 °C (the temperature of coalescence) in (CDCl$_2$)$_2$ from the difference in the resonance frequencies of the exchanging signals ($\Delta \nu = 141$ Hz) using the simple approximation $k_c \approx 2.22 \Delta \nu$. The rate constant of the exchange of the signals of free and complexed TCNB **3** in the ^{1}H NMR spectrum of a 1:2 mixture of **1b** and **3** in [D$_8$]toluene at 60 °C was estimated to be on the same order of magnitude ($k \approx 1000$ s^{-1}, $\Delta G^{\neq} \approx 15.0$ kcal mol^{-1}).

Provided the structure of the TCNB complex of diacetoxy-substituted tweezer **1b** in solution resembles that of the parent tweezer in **3@1a** obtained by single-crystal structure analysis, the TCNB protons are expected to be chemically nonequivalent in complex **3@1b**. This is also true for the complex structure which was calculated by force-field MMFF94[34,35] (Monte Carlo conformer search) to be the energy minimum (Figure 3). In the ^{1}H NMR spectrum of **3@1b** at 25 °C (500 MHz, CD$_2$Cl$_2$, see Supporting Information: Figure S2) the signal for both TCNB protons is evidently superimposed by the aliphatic signals of **1b** and cannot be assigned. By lowering the temperature this signal is broadened and finally split into two signals at $\delta = 2.15$ and 2.35 ppm, as expected for the calculated structures of complex **3@1b**, in which the TCNB molecule adopts a position either with a

tons at the terminal benzene units (H^d, H$^{d'}$, H^e, H$^{e'}$) of empty and complexed **1b**, that is, at room temperature ex-pected for the calculated

a)

b)

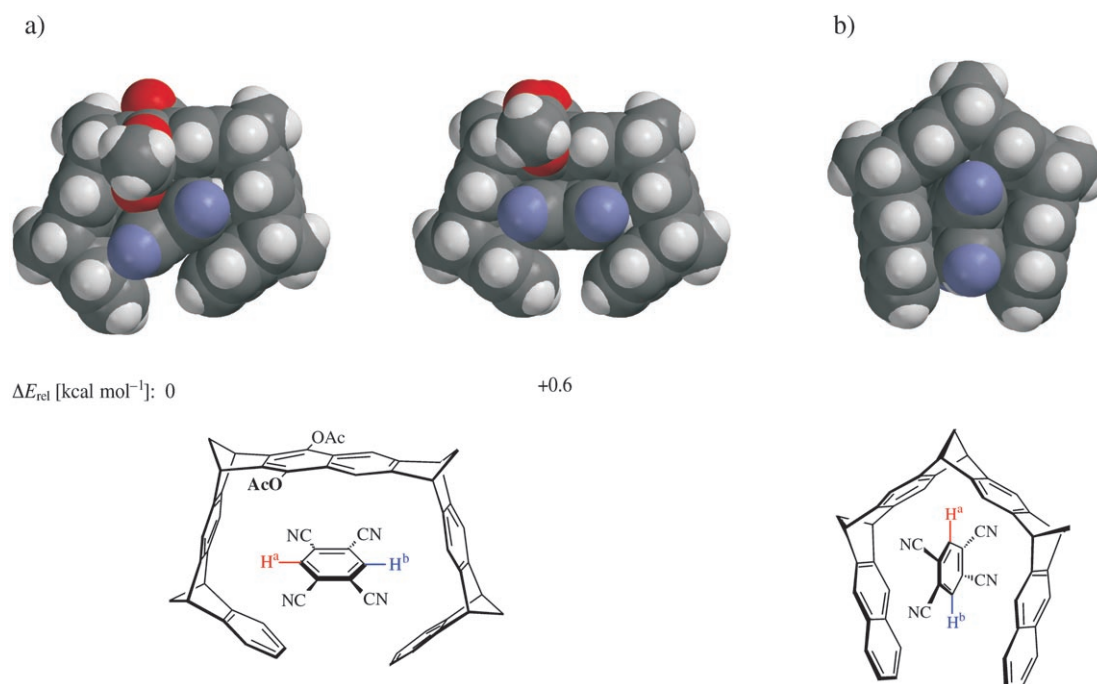ΔE_{rel} [kcal mol^{-1}]: 0   +0.6

Figure 3. The lowest energy structures of a) **3@1b** and b) **3@2a** calculated by force-field MMFF 94[34,35] (Monte Carlo conformer search).

slope or parallel to the diacetoxynaphthalene spacer unit with hydrogen atoms H^a and H^b pointing toward the sidewalls of the tweezer and the cyano groups out of the cavity (Figure 3). The kinetics of "intramolecular" exchange of H^a and H^b inside complex **3@1b** could not be determined by line-shape analysis of the temperature-dependent ^{1}H NMR spectra in CD$_2$Cl$_2$, owing to the overlap of the TCNB signal at $\delta = 2.35$ ppm with those of the CH$_2$ and CH$_3$ protons of **1b** at $\delta = 2.35$ ppm. In the ^{1}H NMR spectrum of **3@1b** in [D$_8$]toluene at -55 °C the signals assigned to TCNB protons H^a and H^b are both shifted downfield, to $\delta = 2.40$ and 2.98 ppm, and do not overlap with signals assigned to the CH$_2$ and CH$_3$ protons of **1b** (Figure 4). In this case the spe-
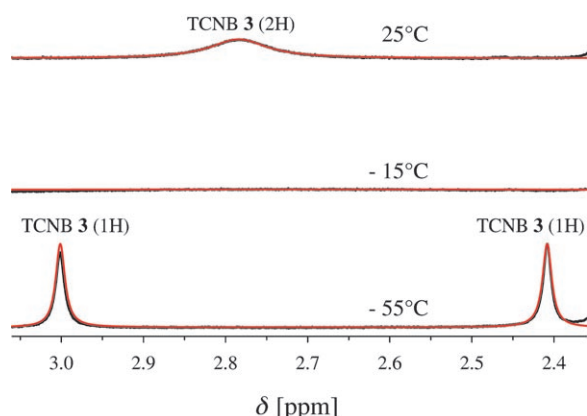
cific rate constants k of the exchange of H^a and H^b inside complex **3@1b** could be determined by line-shape analysis of the temperature-dependent ^{1}H NMR signals (Figure 5a, Table 2a).

The parent trimethylene-bridged clip **2a** forms a highly stable 1:1 complex with TCNB (**3**) besides a weaker 2:1 complex (25 °C: K (1:1) $= 14.3 \times 10^6$ M^{-1} and K (2:1) $= 4.4 \times 10^4$ M^{-1}).[30] The 1:1 complex **3@2a** is even more stable than the corresponding tweezer complex **3@1b** ($K = 7.3 \times 10^5$ M^{-1}).[36] The ^{1}H NMR spectrum of a 2:1 mixture of clip **2a** and **3** (500 MHz, [D$_8$]toluene, 25 °C), however, shows no separate signals for complexed and empty **2a**. Only a specific broadening of the proton signals of **2a** indicates an exchange process that is still fast relative to the NMR time-scale, contrary to the above-mentioned guest exchange between empty and complexed tweezers **1a,b** which is slow at room temperature, so that separate ^{1}H NMR signals of empty and complexed **1a,b** were observed. In the temperature range between $+5$ and -40 °C, exchange between empty and complexed **2a** could be also observed in the ^{1}H NMR spectrum of clip **2a** and **3** (Figure 6), and the specific rate constants at different temperatures (Table 1b), and hence the activation parameters, could be again determined by line-shape analyses (Figure 2b).

In the ^{1}H NMR spectrum of **2a** and TCNB (**3**), further lowering of the temperature ($T < -40$ °C) led to broadening and finally, at -105 °C, to splitting of the TCNB signal into two singlets at $\delta = 2.9$ and 4.4 ppm. The finding of two separated ^{1}H NMR signals for the complexed TCNB protons at -105 °C is good evidence for the complex structure calculated by force-field MMFF 94,[34,35] which is the ground state of **3@2a**. In this structure the plane of the benzene ring of **3** is
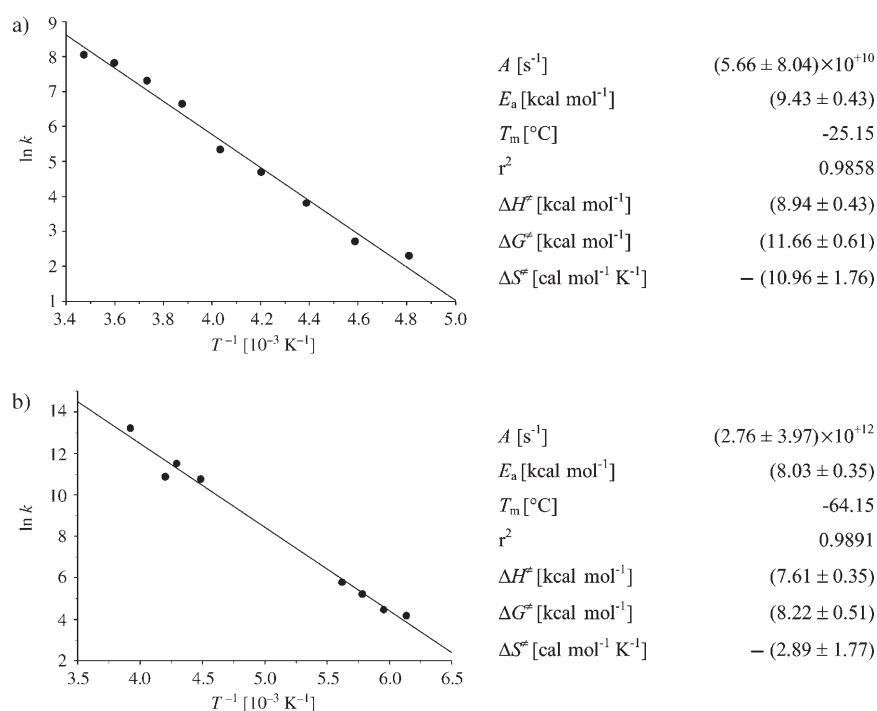

Figure 4. ^{1}H NMR spectra (500 MHz, [D$_8$]toluene) of a 1:1 mixture of clip **1b** and TCNB (**3**) ([**1b**]$_0 = 0.01$ M, [**3**]$_0 = 0.01$ M) at different temperatures. The superimposed red-line fit to the peaks results from line-shape analysis.

a)

A [s^{-1}]	$(5.66 \pm 8.04) \times 10^{+10}$
E_a [kcal mol^{-1}]	(9.43 ± 0.43)
T_m [°C]	-25.15
r^2	0.9858
$\Delta H^{\neq}$ [kcal mol^{-1}]	(8.94 ± 0.43)
$\Delta G^{\neq}$ [kcal mol^{-1}]	(11.66 ± 0.61)
$\Delta S^{\neq}$ [cal mol^{-1} K^{-1}]	$-(10.96 \pm 1.76)$

b)

A [s^{-1}]	$(2.76 \pm 3.97) \times 10^{+12}$
E_a [kcal mol^{-1}]	(8.03 ± 0.35)
T_m [°C]	-64.15
r^2	0.9891
$\Delta H^{\neq}$ [kcal mol^{-1}]	(7.61 ± 0.35)
$\Delta G^{\neq}$ [kcal mol^{-1}]	(8.22 ± 0.51)
$\Delta S^{\neq}$ [cal mol^{-1} K^{-1}]	$-(2.89 \pm 1.77)$

Figure 5. Arrhenius plots ($\ln k$ vs T^{-1} [K^{-1}]) and activation parameters (enthalpy $\Delta H^{\neq}$, entropy $\Delta S^{\neq}$, and Gibbs enthalpy $\Delta G^{\neq}$ of activation) resulting from the temperature dependence of the specific rate constants k listed in Table 2 for exchange of the TCNB protons H^a and H^b inside the cavity of a) **1b**; b) **2a**.

Table 2. Temperature dependence of the specific rate constants k of exchange of protons H^a and H^b of TCNB (**3**) inside the host–guest complex, determined from the line-shape of the exchanging-guest signals in the ^{1}H NMR spectra (500 MHz, [D$_8$]toluene): a) tweezer **1b** and TCNB (**3**); b) clip **2a** and TCNB (**3**).

	a		b
T [°C]	k [s^{-1}]	T [°C]	k [s^{-1}]
-70	1.3	-110	65
-65	10	-105	(87 ± 7)[a]
-55	(17.5 ± 2.5)[a]	-100	(186 ± 6)[a]
-45	45	-95	327
-35	(109 ± 1)[a]	-50	$(47\,000 \pm 3000)$[a]
-25	209	-40	$100\,000$
-15	(735 ± 35)[a]	-35	$53\,000$
-5	(1550 ± 50)[a]	-18	$550\,000$
5	2500		
15	3140		

[a] Rate constants were determined by two independent measurements on TCNB (**3**) and **1b** or **2a** (1:2) and (1:1).

positioned nearly parallel to the naphthalene sidewalls of **2a** with all four TCNB cyano groups pointing out of the clip cavity and H^a, H^b pointing either toward or away from the central norbornadiene spacer unit of **2a** (Figure 3b). The specific rate constants k and activation parameters of the exchange of H^a and H^b of **3** inside complex **3@2a** could be again determined by line-shape analysis of the temperature-dependent ^{1}H NMR signals (Figure 5b and Table 2b). Due to partial overlap of the averaged TCNB signal with one of the bridgehead signals of complexed **2a** (Figure 7) the

errors in the rate constants calculated at temperatures $T < -100\,°C$ from the fit of the line-shape of the TCNB signal are certainly larger than those calculated from the line shapes of the separated TCNB signals at $T < -100$ C. Therefore, in this case the enthalpy and entropy of activation derived from the temperature dependence of the rate constants k is only of little significance, whereas the error in the Gibbs activation enthalpy which can be derived from a k value at a single temperature is certainly much smaller.[37]

The rapid exchange of the ^{1}H NMR signals of the TCNB guest protons H^a and H^b observed in complexes **3@1b** and **3@2a** by ^{1}H NMR spectroscopy at low temperatures can be explained by rotation of the guest molecule inside the tweezer or clip cavity. The activation barri-
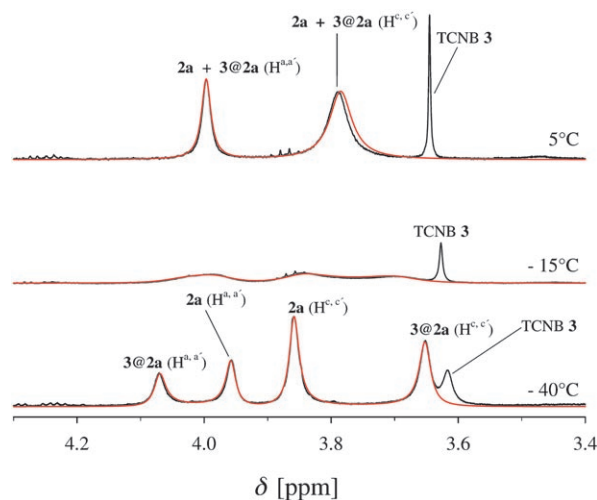

Figure 6. ^{1}H NMR spectra (500 MHz, [D$_8$]toluene) of a 2:1 mixture of clip **2a** and TCNB (**3**) ([**2a**]$_0$ = 0.01 M, [**3**]$_0$ = 0.005 M) at different temperatures. Only the signals assigned to the bridgehead protons of **2a** and complexed **3** [5°C: δ = 3.64 (**3**), 3.79 (**2a**-H^c), and 3.99 (**2a**-H^a); -40°C: δ = 3.65 (**3@2a**-H^c), 4.07 (**3@2a**-H^a), and 3.86 (free **2a**-H^c), 3.96 (free **2a**-H^a)] are shown. The superimposed red-line fit to the peaks results from line-shape analysis.

ers calculated for rotation of the TCNB molecule around the C_2 axis (dividing the bonds C^1–C^2 and C^4–C^5) by force-field MMFF 94[34,35] (Figure 8a, b) are in good agreement with the experimental values. The activation barriers for other rotational processes, in which the TCNB molecule ro-
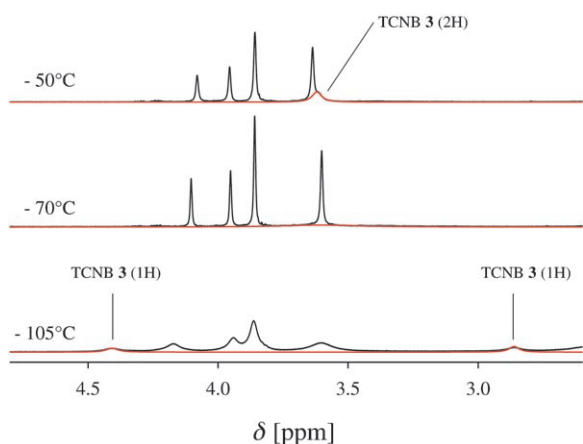
Figure 7. ^{1}H NMR spectra (500 MHz, [D$_8$]toluene) of a 2:1 mixture of clip **2a** and TCNB (**3**) ([**2a**]$_0$ = 0.01 M, [**3**]$_0$ = 0.005 M) at different low temperatures. The superimposed red-line fit to the peaks results from line-shape analysis.

tates around the C_6 axis (through the center of the benzene ring) and the cyano groups must move through the host

cavity, are calculated to be much higher than the experimental data.[38] The rotation of the TCNB molecule inside the tweezer or clip cavity in complexes **3@1b** and **3@2a** can be considered to be the dynamic equilibration of noncovalent conformers. Comparison with the rotational barriers of conformers covalently bound by C−C σ bonds, for example, ethane or *n*-butane, shows that the rotation in the noncovalent conformers is even more hindered than in covalently bound conformers.

Besides rapid guest rotation inside the host cavity, the TCNB complexes of the molecular tweezers and clips **3@1a,b** and **3@2a** are kinetically and thermodynamically very stable. Exchange of the guest molecule between the host–guest complex and the empty host molecule observed by temperature-dependent ^{1}H NMR spectroscopy can be the result either of complete dissociation and reformation of the host–guest complex (Figure 9, path a) or associative, S$_N$2-like host–guest exchange (Figure 9, path b). Therefore, the complex dissociation barriers are either equal to or even higher than the experimentally determined activation parameters of the exchange of the guest molecule between the host–guest complex and the empty host.
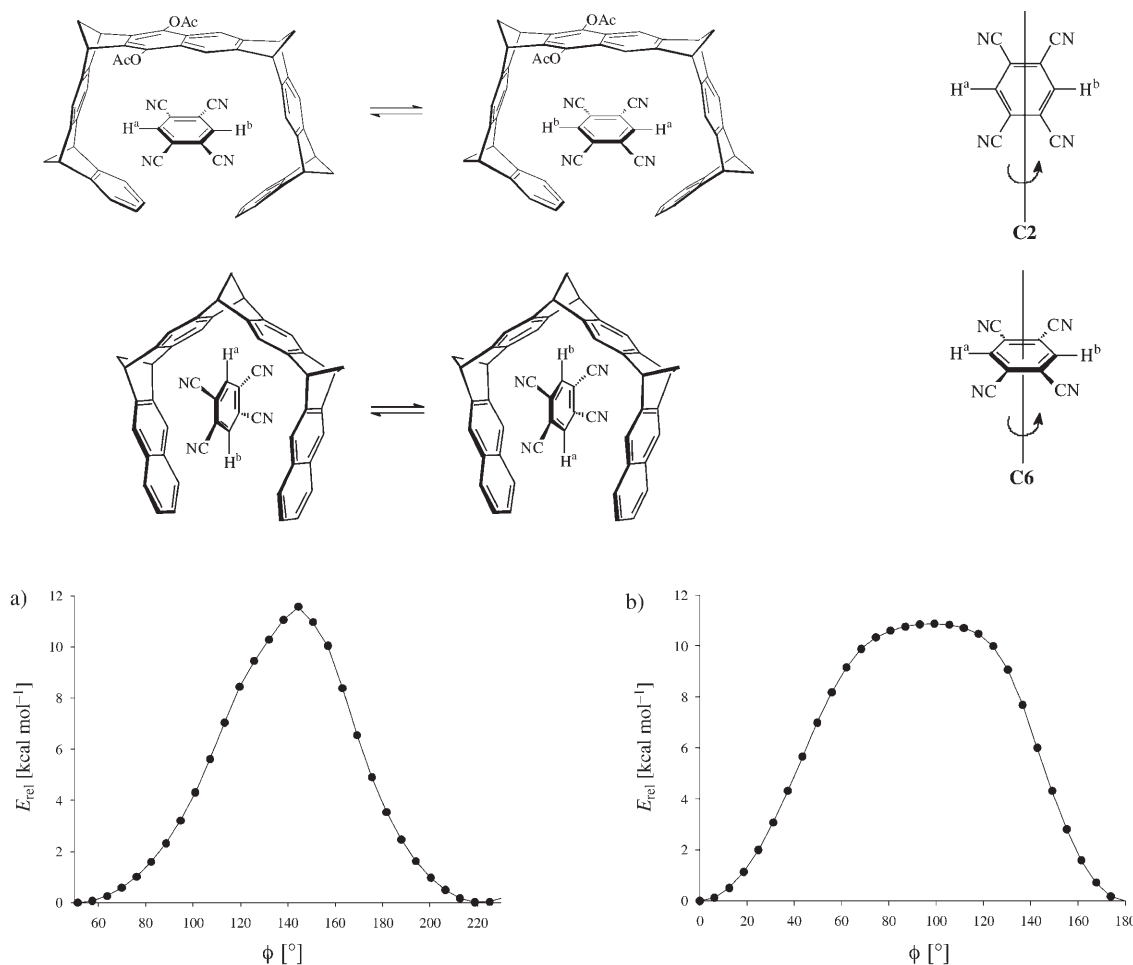

Figure 8. Activation barriers of rotation of TCNB (**3**) inside the cavity of a) **1a** and b) **2a** (both around the C_2 axis) calculated by force-field MMFF94.[34,35]
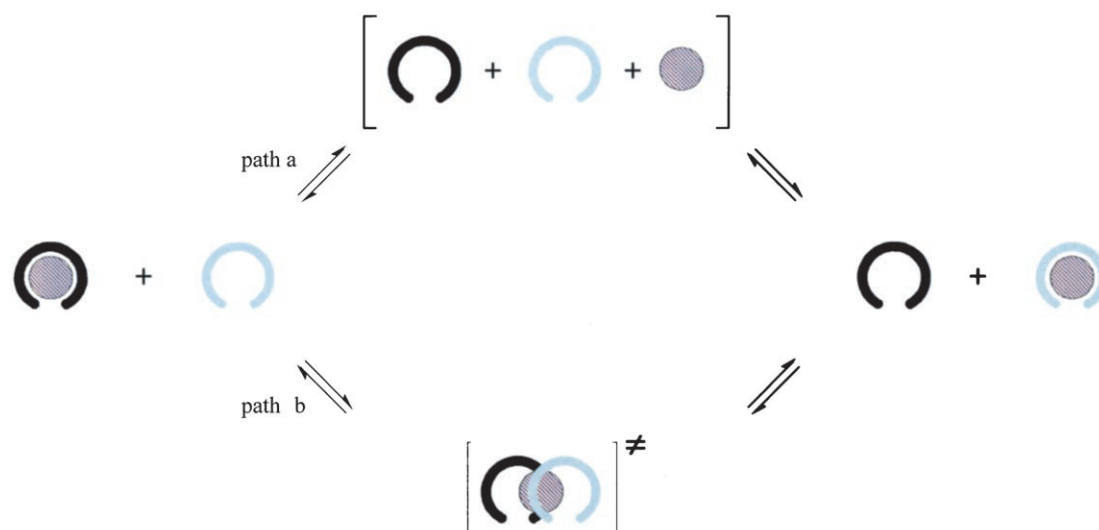
Figure 9. Schematic presentation of the exchange of a guest molecule between a host–guest complex and an empty host molecule a) by a dissociative and b) by an associative S_N2-like mechanism.

The finding that the rate constant of the dissociation of complex **3@1b** determined independently by cyclic voltammetry experiments performed at different scan rates ($k = 200\,s^{-1}$ at room temperature)[36] is on the same order of magnitude as that observed for the exchange of TCNB (**3**) between complex **3@1b** and empty tweezer **1b** by temperature-dependent ^1H NMR ($k = 313\,s^{-1}$ at 60°C) suggests that the latter process also occurs by the dissociative mechanism (Figure 9, path a). The observation of negative entropies of

activation, however, seems to support the associative mechanism, but this can be also explained with the dissociative mechanism. In the transition states of the dissociation of complex **3@1a** and **3@2a** calculated by force-field MMFF 94, guest rotation inside the host cavity must be restricted, and the guest molecule **3** is still clipped between the tips of **1a** or **2a** (Figure 10). Both processes—restriction of rotational and translatory degrees of freedom—contribute negative terms to the entropy of activation.
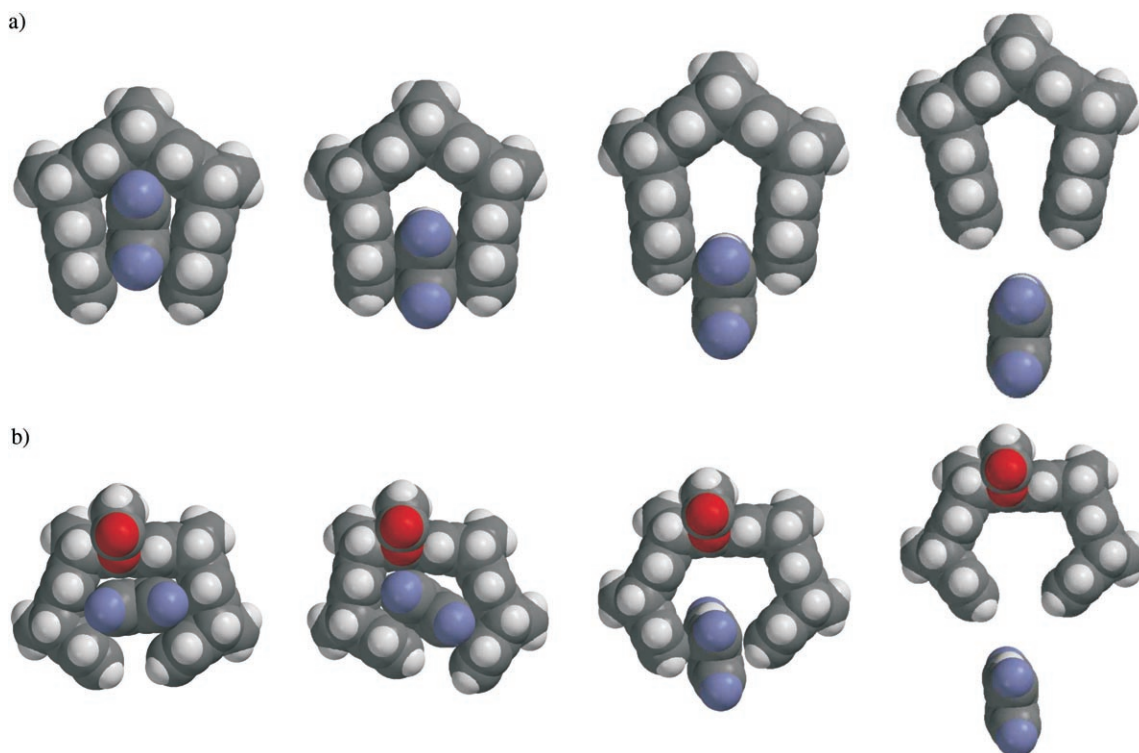

Figure 10. Schematic description of complex dissociation via path a: a) **3@2a**; b) **3@1b** (calculated by force-field MMFF94).[34,35]

Complex formation between TCNB (**3**) and tweezer **1b** or clip **2a** can be further characterized by the construction of complete Gibbs enthalpy diagrams for complex association/dissociation (Figures 11 and 12) by means of the now-
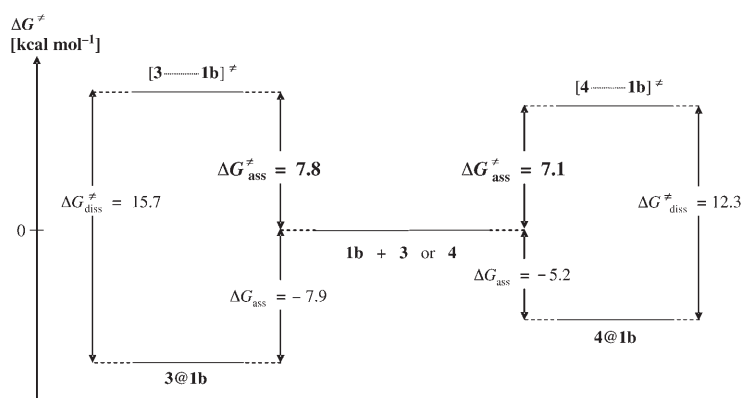
$\Delta G^{\neq}$
[kcal mol^{-1}]

[3⋯⋯1b]$^{\neq}$

[4⋯⋯1b]$^{\neq}$

$\Delta G^{\neq}_{ass} = 7.8$ $\Delta G^{\neq}_{ass} = 7.1$

$\Delta G^{\neq}_{diss} = 15.7$

$\Delta G^{\neq}_{diss} = 12.3$

1b + 3 or 4

$\Delta G_{ass} = -5.2$

$\Delta G_{ass} = -7.9$

4@1b

3@1b

Figure 11. Gibbs enthalpy diagram of association and dissociation of the complexes of tweezer **1b** with TCNB (**3**)[39] (left) and tropylium tetrafluoroborate (**4**, right).

$\Delta G^{\neq}$
[kcal mol^{-1}]

[3⋯⋯2b]$^{\neq}$

[3⋯⋯2a]$^{\neq}$

$\Delta G^{\neq}_{ass} = 5.2$

$\Delta G^{\neq}_{ass} = 2.9$

$\Delta G^{\neq}_{diss} = 12.4$

$\Delta G^{\neq}_{diss} = 11.2$

2a or 2b + 3

$\Delta G_{ass} = -6.0$

$\Delta G_{ass} = -9.5$

3@2b

3@2a
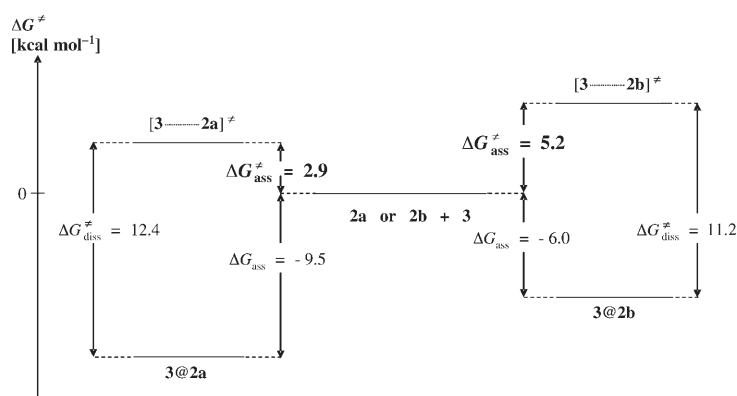
Figure 12. Gibbs enthalpy diagram of the association and dissociation of the complexes of clips **2a** (left) and **2b** (right) with TCNB (**3**).[39]

available kinetic and thermodynamic data. From these diagrams it becomes evident that complex formation between **3** and tweezer **1b** has a substantial activation barrier, whereas the activation barrier for formation of complex **3@2a** is small (not far from a diffusion-controlled process). These findings can be explained by the different topologies of tweezers **1a,b** and clip **2a**. The tweezers have the topology of an almost closed wheel, which requires substantial expansion of the tweezer's tips in the transition state of complex formation and makes the inclusion of the guest molecule inside the cavity a kinetically rather difficult process, whereas clip **2a** has a much more open topology which makes the inclusion of the guest molecule easier and hence the activation barrier for this process smaller. The same arguments can be applied to explain the activation barrier of guest rotation inside the host cavity, which is higher in tweezer complex **3@1b** than in clip complex **3a@2a**.

In complexes **3@1a,b** and **3@2a** the cyano groups of the TCNB guest molecule, which point out of the cavity at the open tweezer or clip faces, evidently prevent complex dissociation by guest departure through the open tweezer or clip face and force the guest molecule to leave the cavity through the host's tips. To make this second pathway accessible, too, and to find out whether the association proceeds under diffusion control in this case, we studied complex formation between diacetoxy-substituted tweezer **1b** and tropylium tetrafluoroborate (**4**). In the 500 MHz ^{1}H NMR spectrum of a 2:1 mixture of **1b** and **4** in CDCl$_3$/CD$_3$OD (1:1), in which both components are soluble, at 25°C the sharp singlet assigned to the protons of **4** is shifted upfield by $\Delta\delta_{obs} = 3.13$ ppm. The signals at $\delta = 6.4$ and 6.5 ppm, assigned to the protons at one of the terminal benzene rings of **1b**, are already broadened, and this indicates fast exchange of guest molecule **4** between complex **4@1b** and empty tweezer **1b**. An increase in temperature ($T > 25$°C) leads to sharpening of the tweezer signals, whereas a decrease in temperature ($T > 25$°C) leads to further broadening and finally, at -50°C, to splitting of these signals into three signals at $\delta = 6.0$, 6.1, and 6.8 ppm which could be assigned to complex **4@1b** and empty **1b**, respectively. At -50°C exchange is slow, and from the ^{1}H NMR signal assigned to the protons of **4** a maximum complexation-induced shift of the guest protons of $\Delta\delta_{max} = 3.22$ ppm could be obtained (Supporting Information: Figure S3). The sharp ^{1}H NMR signal observed for complexed **4** at -50°C indicates that guest rotation inside the tweezer cavity is still fast with respect to the NMR timescale. The binding constant of the formation of complex **4@1b** at 25°C can be calculated by use of the starting concentrations $[\mathbf{1b}]_0 = 0.01$ M and $[\mathbf{4}]_0 = 0.005$ M and the complexation-induced shifts $\Delta\delta_{obs}$ and $\Delta\delta_{max}$ to be $K_a = 6750$ M^{-1}. The specific rate constants k and activation parameters of the exchange of guest **4** between complex **4@1b** and empty tweezer **1b** could again be determined by line-shape analysis of the temperature-dependent ^{1}H NMR spectra (Table 1c, Figure 2c). By using the kinetic and thermodynamic data, the Gibbs enthalpy diagram can be constructed for complex formation between **4** and tweezer **1b** (Figure 11, right). Accordingly, the dissociation barrier of complex **4@1b** ($\Delta G^{\neq} = 12.3$ kcal mol^{-1}) is significantly smaller than those of the TCNB–tweezer complexes **3@1a,b** ($\Delta G^{\neq} = 16.8$ and 15.7 kcal mol^{-1}, respectively) and of similar size to that of TCNB–clip complex **3@2a** ($\Delta G^{\neq} = 12.4$ kcal mol^{-1}). This comparison of the dissociation barriers, however, does not allow any conclusion concerning the question whether the formation of tropylium complex **4@1b** proceeds differently to that of TCNB complex **3@1b**, because all these complexes are of different thermodynamic stability, and this contributes to the size of the dissociation barrier. The association barriers provide the answer to this question. They are calculated from the experimental kinetic and thermodynamic data to be $\Delta G^{\neq} = 7.8$ and 7.1 kcal mol^{-1}, respectively (Figure 11), and thus of very similar size to those for formation of tweezer complexes **3@1b** and **4@1b**. These barriers are significantly larger than that calculated for clip

complex **3@2a** ($\Delta G^\ddagger = 2.8$ kcal mol^{-1}, Figure 12). This finding is good evidence that formation of tropylium complex **4@1b** proceeds similarly to that of TCNB complex **3@1b** by picking up the guest molecule through the tips of the tweezer. This suggestion is further supported by the finding of a negative activation entropy of dissociation of **4@1b**, comparable to those of **3@1a** and **3@2a**.

If complex formation indeed occurs as suggested, by entry of the guest molecule into the cavity through the host tips, substituents at the tips are expected to affect the size of the association barrier. To determine the effect of such substituents we synthesized and investigated the hitherto-unknown tetrabromo-substituted clip **2b** (Scheme 1). Clip **2b** can be

of the central (H^g) and peripheral methylene bridges (H^h), respectively, two signals at $\delta = 4.0$ (H^c) and 4.1 ppm (H^a) in a 2:1 ratio for the bridgehead protons, and three singlets at $\delta = 6.7$, 7.1 and 7.2 ppm in a 2:2:2 ratio for the remaining aromatic protons (H^e, H^d, H^b) at the benzene and naphthalene rings. The ^{1}H NMR signals of **2b** show concentration-dependent shifts indicating a self-association process (for details, see Supporting Information). The specific broadening of the singlets at $\delta = 6.7$ (H^e) and 7.1 ppm (H^d) assigned to the naphthalene protons indicates that the naphthalene sidewalls are involved in this self-association of **2b**.

Tetrabromo-substituted clip **2b** forms host–guest complexes with TCNB (**3**), TCNQ (**12**), and TNF (**13**). Complex
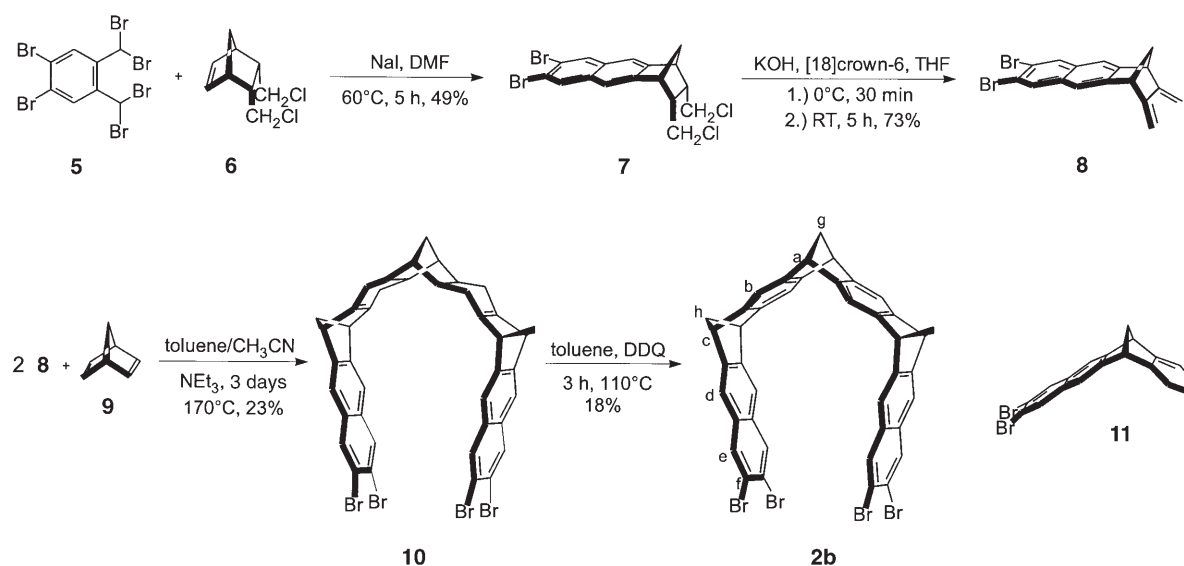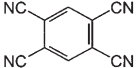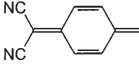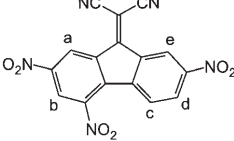

Scheme 1. Synthesis of tetrabomo-substituted clip **2b**.

prepared analogously to parent clip **2a**[30] starting from hexabromo-*o*-xylene **5**[40,41] and 5,6-bis(chloromethyl)norbornene (**6**).[42–44] 1,4-Br$_2$ elimination of **5** by sodium iodide generates the unstable tetrabromo-*o*-quinodimethane, which reacts further with norbornene **6** in the fashion of a Diels–Alder cycloaddition followed by twofold HBr elimination in the primary cycloadduct to produce naphthonorbornene **7**. Basic HCl elimination from **7** leads to diene **8**. Repetitive Diels–Alder reactions of diene **8** with norbornadiene **9** as bis-dienophile proceeded stereoselectively on the *endo* face of the diene and the *exo* face of the bis-dienophile to give all-*syn* bis-adduct **10**, which was converted to the desired tetrabromo-substituted clip **2b** by oxidative dehydrogenation with 2,3-dichloro-5,6-dicyano-1,4-benzoquinone (DDQ). In the last step benzonaphthonorbornadiene **11** was observed as byproduct which can be explained by a retro-Diels–Alder reaction of a partially dehydrogenated primary product in the DDQ oxidation of **10**. The symmetric structure of **2b** can be unambiguously assigned from its ^{1}H NMR spectrum (500 MHz, CDCl$_3$), which displays a singlet at $\delta = 2.5$ and an AB spectrum at $\delta = 2.3$, 2.4 for the CH$_2$ protons

formation could be easily detected by the characteristic upfield shifts of the signals of the guest protons. No complexation could be detected by this NMR criterion for *p*-dinitrobenzene, *p*- and *m*-dicyanobenzene, 1,5-difluoro-2,4-dinitrobenzene, or 1-ethyl-4-(methoxycarbonyl)pyridinium iodide (Kosower salt) as guest molecules. The maximum complexation-induced shifts $\Delta\delta_{max}$, the association constants K_a, and hence the Gibbs enthalpies ΔG of association could be determined for the formation of complexes of **2b** with **3**, **12**, and **13** by ^{1}H NMR titration experiments (Table 3). Clip **2b** forms the most stable, bright yellow complex with **3**. The yellow color of the complex results from a charge transfer (CT) absorption band at $\lambda_{max} = 405$ nm ($\varepsilon = 789$, CHCl$_3$). The association constant K_a of formation of **3@2b** and the thermodynamic parameters ΔH, ΔS, and ΔG could be determined by use of an isothermal titration microcalorimeter (ITC, Figure 13). The values of K_a and ΔG derived from the calorimetric measurements agree well with those obtained independently by ^{1}H NMR titration experiments (Table 4).

The TCNB and TCNQ complexes of tetrabromo-substituted clip **2b** are substantially less stable, by a factor of 560

Table 3. Comparison of $\Delta\delta_{max}$, K_a [M^{-1}], and ΔG [kcal mol^{-1}] for the formation of complexes between clips **2a** and **2b** as host molecule and guest molecules **3**, **12**, and **13** in CDCl$_3$ at 25°C.

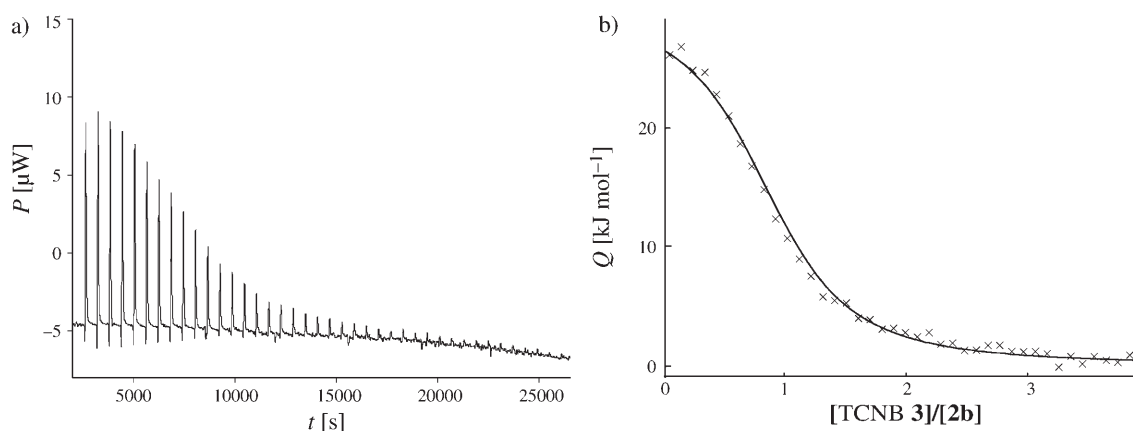|	Host					
	2b			**2a**		
Guest	$\Delta\delta_{max}$	K_a	ΔG	$\Delta\delta_{max}$	K_a	ΔG
(structure)	4.6	$25\,600 \pm 520$	-6.0	4.7	$(14.3\pm0.3)\times10^6$ (1:1)[a]	-9.8
					$(4.4\pm0.9)\times10^4$ (2:1)[a]	-6.3
(structure)	1.9	1300 ± 100	-4.0	3.3	2600 ± 150	-4.6
(structure)	0.6 (H^a)			1.1 (H^a)		
	1.8 (H^b)			1.5 (H^b)		
	2.0 (H^c)	940 ± 40	-4.0	4.6 (H^c)	130 ± 10	-2.9
	2.0 (H^d)			4.0 (H^d)		
	0.6 (H^e)			2.1 (H^e)		

[a] ITC measurement.

Figure 13. a) Plot of the experimental calorimetric data: Measured power versus time. b) Analysis of the experimental data: Heat of reaction versus concentration ratio [**3**]/[**2b**].

Table 4. Thermodynamic data for formation of complex **3@2b** calculated from calorimetric measurements.

K_a [M^{-1}]	ΔG [kcal mol^{-1}]	ΔH [kcal mol^{-1}]	ΔS [cal mol^{-1} K^{-1}]
$26\,500 \pm 2000$	-6.0[a]	-7.1	-3.7

and 2, respectively, than the corresponding complexes of parent clip **2a**, whereas the TNF complex **13@2b** is more stable by a factor of 7.2 than **13@2a** (Table 3). These results can be explained by the effect of the bromo substituents on the electrostatic potential surface (EPS) and the van der-Waals contact surface of clip **2b**. Evidently, binding of relatively small but highly electron deficient guest molecules such as TCNB (**3**) and TCNQ (**12**) to clips **2a,b** is predominantly electrostatic in nature. Due to the electron-withdrawing bromo substituents, the EPS inside the cavity of **2b** is less negative than that of **2a**,[45] and hence complexes **3@2b** and **12@2b** are less stable than **3@2a** and **12@2a**. In the case of TNF (**13**) with its extended aromatic π system, the dispersion forces are more important for host–guest binding.

That explains why clip **2b**, with its larger van der Waals contact surface, forms a more stable complex with **13** than **2a** (Figure 14).

The specific rate constants k and the activation parameters of the dissociation of complex **3@2b** could again be determined by line-shape analysis of the temperature-dependent ^{1}H NMR spectra of a (2:1) mixture of clip **2b** and TNCB **3** (Table 1 d, Figure 2 d; Supporting Information: Figure S4). The complete Gibbs enthalpy diagram (Figure 12, right), constructed from kinetic and thermodynamic measurements, clearly shows that the Gibbs activation enthalpy calculated for the formation of complex **3@2b** of $\Delta G_{ass}^{\neq} = 5.2$ kcal mol^{-1} is significantly larger than that of the formation of **3@2b** ($\Delta G_{ass}^{\neq} = 2.9$ kcal mol^{-1}), as is expected for the entry of the guest molecule into the host cavity through its tips.

Conclusion

Analysis of the dynamics in host–guest complexes of molecular tweezers **1a,b** and clips **2a,b** with TCNB (**3**) and tropy-
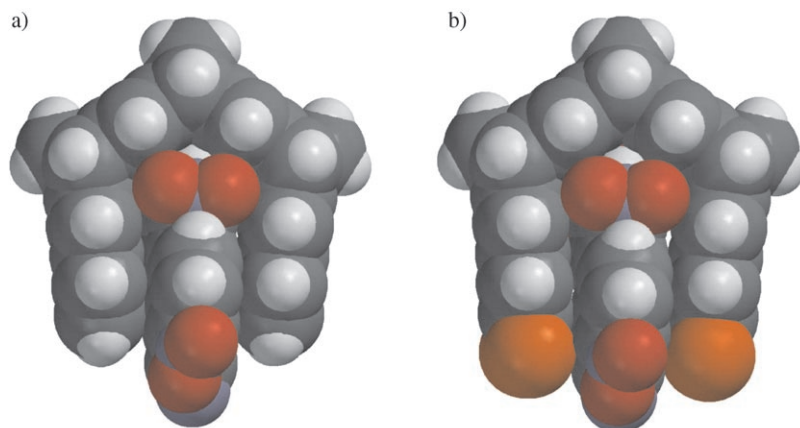
Figure 14. Geometries of the TNF complexes a) **13@2a** and b) **13@2b** calculated by force-field MMFF94.[34,35]

lium tetrafluoroborate (**4**) by temperature-dependent ^{1}H NMR spectroscopy allows the conclusion that complex formation proceeds by clipping of the guest molecule between the tips of the tweezers before it moves into its final position inside the host cavity. In the ^{1}H NMR spectra of **3@1b** and **3@2a** at very low temperatures, we could observe that **3** undergoes fast rotation inside the cavity of tweezer **1b** or clip **2a**. In the TCNB complex of parent tweezer **1a**, guest rotation certainly occurs at a rate comparable to that in complex **3@1b**, but this process cannot be experimentally detected because the two TCNB protons remain chemically and hence magnetically equivalent in the complex **3@1a**. In the clip complex **3@2a** the association and rotational barriers are smaller by $\Delta\Delta G^\ddagger = 3$–4 kcal mol^{-1} than those in tweezer complexes **3@1a,b**. This can be explained by the more open topology of the trimethylene-bridged clips compared to that of the tetramethylene-bridged tweezers. Finally, the bromo substituents in the newly prepared clip **2b** have a substantial effect on the kinetics and thermodynamics of complex formation. Clip **2b** forms weaker complexes with **3** and TCNQ (**12**) and a more stable complex with TNF (**13**) than parent clip **2a**. These results can be explained by a less negative EPS and a larger van der Waals contact surface of **2b** compared to **2a**.

Experimental Section

General: IR: Bio-Rad FTS 135. UV: Varian Cary 300 Bio. ^{1}H NMR, ^{13}C NMR, DEPT, H,H-COSY, C,H-COSY, NOESY, HMQC, HMBC: Bruker DRX 500; ^{1}H NMR titration experiments: Varian Gemini XL 200 and Bruker DRX 500; the undeuterated residue of the solvent was used as internal standard. Positions of the protons of the methano bridges are indicated by the letters *i* (*innen*, towards the center of the molecule) and *a* (*aussen*, away from the center of the molecule). MS: Fison Instruments VG ProSpec 3000 (70 eV). All melting points are uncorrected. Thin-layer chromatography (tlc): Polygram SIL G/UV$_{254}$ 0.2 mm silica gel with fluorescent indicator. Column chromatography: silica gel 0.063–0.2 mm. All solvents were distilled prior to use. Ampoules were sealed in vacuo after three freeze (2-propanol/dry ice) and thaw cycles with argon as inert gas. Microcalorimetry experiments: All titration experiments were performed on a TAM 2277 microcalorimeter (Thermometric, Järfäl-

la, Sweden) using the ampoule unit 2277-201. The temperature during the experiments was 298 K and we used chloroform as solvent. 1 mL of the receptor solution was filled into the cell of the microcalorimeter. The addition of the substrate solution during the titration experiment was managed with a syringe-pump 6120-031, Lund, Sweden.

***cis*-2,3-Bis(chloromethyl)-1,2,3,4-methano-1,2,3,4-tetrahydro-6,7-dibromoanthracene (7)**: Powdered sodium iodide (80 g) was added in one portion to a stirred solution of hexabromoxylene **5**[40,41] (41 g, 70.0 mmol) and dienophile **6**[42–44] (6 g, 31.0 mmol) in anhydrous DMF (300 mL) at 60°C under argon. The mixture was stirred for 5 h and then poured into ice water (600 mL). Saturated aqueous NaHSO$_3$ was added to the brownish mixture until its color turned to light yellow. The resulting precipitate was dissolved in dichloromethane (300 mL) and the separated organic phase was washed with saturated aqueous NaHCO$_3$, water, and dried over anhydrous MgSO$_4$. After removal of the solvent the crude product was purified by column chromatography (silica gel, cyclohexane/ethyl acetate 10/1) to give **7** as a beige solid (6.8 g, 15 mmol, 49%). tlc: R_f (cyclohexane/ethyl acetate 10/1): 0.67; m.p. 137°C; ^{1}H NMR (500 MHz, CDCl$_3$): $\delta = 1.89$ (d, 1 H, ^2J(13a-H, 13i-H) = 9.6 Hz, 13a-H), 1.99 (d, 1 H, ^2J(13i-H, 13a-H) = 9.6 Hz, 13i-H), 2.57 (m, 2 H, 11-H/12-H), 2.84 (m, 2 H, 2-H, 3-H), 3.21 (m, 2 H, 11-H/12-H), 3.67 (s, 2 H, 1-H, 4-H), 7.57 (s, 2 H, 9-H, 10-H), 8.08 ppm (s, 2 H, 5-H, 8-H); ^{13}C NMR (126 MHz, CDCl$_3$): $\delta = 43.61$ (t, C-11, C-12), 44.35 (d, C-2, C-3), 46.96 (t, C-13), 47.43 (d, C-1, C-4) , 120.35 (d, C-9, C-10), 121.35 (s, C-6, C-7), 132.04 (d, C-1, C-4), 132.50 (s, C-8a, C-10a), 143.68 ppm (s, C-4a, C-9a); IR (KBr): $\tilde{\nu} = 2989$ (CH), 2944 (CH), 2876 (CH), 1642 (C=C), 1581 (C=C), 1400 (CH$_2$), 1033 (CBr), 900 (CH), 729 cm^{-1} (CCl); UV/Vis (CHCl$_3$): λ_{max} (lg ε) = 275 (3.81), 285 (3.76), 316 (3.13), 330 nm (3.13); MS (70 eV): m/z (%): 448 (84) [M^+], 324 (100) [$M^+-C_4H_4Cl_2$], 243 (90) [$M^+-C_4H_4Cl_2Br$], 163 (76) [$M^+-C_4H_4Cl_2Br_2$]; HRMS (70 eV) calcd (C$_{17}$H$_{14}$Cl$_2$Br$_2$): 445.8839; found: 445.8901.

2,3-Bis-*exo*-methylene-1,4-methano-1,2,3,4-tetrahydro-6,7-dibromoanthracene (8): Under argon at 0°C potassium hydroxide (6 g, 0.11 mol) was added in portions to a solution of [18]crown-6 (300 mg, 1.13 mmol) and **7** (1.8 g, 4.0 mmol) in tetrahydrofuran (60 mL). The mixture was stirred for 30 min at 0°C. After 5 h stirring at room temperature the mixture was poured into ice water (60 mL). The aqueous phase was extracted with diethyl ether (2×60 mL), and the combined organic phases were washed with water and dried over anhydrous MgSO$_4$. After removal of the diethyl ether the crude product was purified by column chromatography (silica gel, *n*-hexane/chloroform 4/1) to give diene **8** as a beige solid (1.12 g, 2.95 mmol, 73%). tlc: R_f (cyclohexane/ethyl acetate 3/1): 0.90; m.p. 143°C; ^{1}H NMR (500 MHz, CDCl$_3$): $\delta = 2.03$ (d, 1 H, ^2J(13a-H, 13i-H) = 8.9 Hz, 13a-H), 2.11 (d, 1 H, ^2J(13i-H, 13a-H) = 8.9 Hz, 13i-H), 3.95 (s, 2 H, 1-H, 4-H), 5.10 (s, 2 H, 11a-H, 12a-H), 5.22 (s, 2 H, 11i-H, 12i-H), 7.46 (s, 2 H, 9-H, 10-H), 7.99 ppm (s, 2 H, 5-H, 8-H); ^{13}C NMR (126 MHz, CDCl$_3$): $\delta = 50.43$ (t, C-13), 52.21 (d, C-1, C-4), 103.02 (t, C-11, C-12), 117.78 (d, C-9, C-10), 120.90 (s, C-6, C-7), 131.94 (d, C-5, C-8), 132.70 (s, C-8a, C-10a), 146.32 (s, C-4a, C-9a), 147.86 ppm (s, C-2, C-3); IR (KBr): $\tilde{\nu} = 3160$ (CH), 3076 (CH$_2$), 2988/2959/2933 (CH$_2$), 2858 (CH), 1633 (C=C), 1583 (C=C), 1469 (CH), 1400 (CH$_2$), 1102 (CBr), 886 cm^{-1} (CH); UV/Vis (CHCl$_3$): λ_{max} (lg ε) = 318 (3.25), 333 nm (3.33); MS (70 eV): m/z (%): 376 (100) [M^+], 216 (60) [M^+-Br_2], 163 (38) [$M^+-C_4H_4Br_2$]; HRMS (70 eV): calcd (C$_{17}$H$_{12}$Br$_2$): 373.9306; found: 373.9294.

2,3,13,14-Tetrabromo-6,7,7a,8,8a,9,10,17,18,18a,19,19a,20,21-tetradecahydro-6,21:8,19:10,17-trimethanononacene (10): A solution of diene **8** (1.12 g, 2.95 mmol), bis-dienophile **9** (106 mg, 1.20 mmol), and anhydrous triethylamine (fifteen drops) in a mixture of anhydrous toluene (8 mL) and anhydrous acetonitrile (2 mL) saturated with argon was heated to

170 °C for three days in a sealed ampoule. The reaction mixture was cooled overnight in a refrigerator. The precipitated product was filtered off, washed thoroughly with cold toluene, and dried in vacuo. The brownish product **10** (200 mg, 0.27 mmol, 23 %) was used without further purification. At room temperature **10** is unstable and decomposes within 24 h. Therefore, **10** must be used for the next step immediately. ^{1}H NMR (500 MHz, CDCl$_3$): $\delta = 1.41$ (m, 4H, 7a-H, 8a-H, 18a-H, 19a-H), 1.55 (s, 2H, 8-H, 19-H), 2.10–2.26 (m, 14H, 7-H$_2$, 8-H, 8-H$_2$, 18-H$_2$, 19-H, 23-H$_2$, 24-H$_2$, 25-H$_2$), 3.60 (s, 4H, 6-H, 10-H, 17-H, 21-H), 7.26 (s, 4H, 1-H, 4-H, 12-H, 15-H), 7.85 ppm (s, 4H, 5-H, 11-H, 16-H, 22-H). The ^{13}C shifts were not assigned due to the low solubility and the long acquisition time for a ^{13}C NMR spectrum with respect to the instability of **15** and and slight contamination by polymers.

2,3,13,14-Tetrabromo-6,8,10,17,19,21-hexahydro-6,21:8,19:10,17-trimethanonononacene (2b): DDQ (350 mg, 0.95 mmol) was added to a solution of **10** (200 mg, 0.24 mmol) in anhydrous toluene (20 mL). The intensively stirred mixture was placed immediately in an oil bath preheated to 110 °C and kept at 110 °C for 3 h. The reaction mixture was allowed to cool to 50 °C. Excess DDQ was converted to DDQH$_2$ by reaction with 1,4-cyclohexadiene (0.2 mL). After stirring for 15 min at 50 °C the mixture was filtered and the filtrate was concentrated in vacuo. Purification of the crude product by column chromatography (silica gel, n-hexane/chloroform 4/1) yielded **2b** as a light yellow solid (42 mg, 0.05 mmol). For further purification the solid was suspended in a small amount of ethyl acetate and treated for 5 min with ultrasound, the solvent was filtered off, and the remaining product was dried in vacuo. Clip **2b** (36 mg, 0.043 mmol, 18 %) was obtained as a colorless solid. tlc: R_f (n-hexane/CHCl$_3$ 4/1): 0.14; m.p. >280 °C (decomp); ^{1}H NMR (500 MHz, CDCl$_3$): $\delta = 2.28$ (d, 2H, ^2J(23i-H, 23a-H) = 8.0 Hz, 23i-H, 25i-H), 2.44 (d, 2H, ^2J(23a-H, 23i-H) = 8.0 Hz, 23a-H, 25a-H), 2.49 (s, 2H, 24-H$_2$), 4.02 (s, 4H, 6-H, 10-H, 17-H, 21-H), 4.09 (s, 2H, 8-H, 19-H), 6.66 (br s, 4H, 1-H, 4-H, 12-H, 15-H), 7.17 (s, 4H, 7-H, 9-H, 18-H, 20-H), 7.21 ppm (br s, 4H, 5-H, 11-H, 16-H, 22-H); ^{13}C NMR (126 MHz, CDCl$_3$): δ [ppm] = 50.82 (d, C-6, C-10, C-17, C-21), 51.66 (d, C-8, C-19), 65.60 (t, C-23, C-25), 69.45 (t, C-24), 116.26 (d, C-7, C-9, C-18, C-20), 117.30 (d, C-1, C-4, C-12, C-15), 120.03 (s, C-2, C-3, C-13, C-14), 130.99 (s, C-4a, C-11a, C-15a, C-22a), 131.37 (d, C-5, C-11, C-16, C-22), 145.93 (s, C-5a, C-10a, C-16a, C-21a), 147.89 (s, C-7a, C-8a, C-18a, C-19a), 148.21 ppm (s, C-6a, C-9a, C-17a, C-20a); IR (KBr): $\tilde{\nu} = 3054$ (CH), 2977/2935 (CH$_2$), 2862 (CH), 1582 (C=C), 1470/1455 (CH), 1404 (CH$_2$), 1104 (CBr), 901 cm^{-1} (CH); UV/Vis (CHCl$_3$): λ_{max} (lg ε) = 286 (4.24), 321 (3.53), 335 nm (3.60); MS (70 eV) m/z (%): 836 (100) [M^+], 756 (24) [M^+–Br], 676 (14) [M^+–Br$_2$], 378 (24) [M^+–C$_{16}$H$_6$Br$_2$], 257 (49) [M^+–C$_{25}$H$_{19}$Br$_2$]; HRMS (70 eV) calcd (C$_{41}$H$_{24}$Br$_4$): 831.8544; found: 831.8548.

Determination of K_a by ^{1}H NMR titration method: Receptor R and substrate S are in equilibrium with the 1:1 complex RS (R + S⇌RS). The association constant K_a is then defined by Equation (1). [R]$_0$ and [S]$_0$ are the starting concentrations of the receptor and the substrate, respectively.

$$K_a = \frac{[RS]}{[R][S]} = \frac{[RS]}{([R]_0-[RS])([S]_0-[RS])} \tag{1}$$

The observed chemical shift δ_{obs} of the substrate in the ^{1}H NMR spectrum is an averaged value between free (δ_0) and complexed substrate (δ_{RS}), assuming that the exchange is fast on the NMR timescale [Eq. (2)]. Combination of Equations (1) and (2) and the use of differences in chemical shift ($\Delta\delta = \delta_0 - \delta_{obs}$; $\Delta\delta_{max} = \delta_0 - \delta_{RS}$) leads to Equation (3).

$$\delta_{obs} = \frac{[S]}{[S]+[RS]}\delta_0 + \frac{[RS]}{[S]+[RS]}\delta_{RS} \tag{2}$$

$$\Delta\delta = \frac{\Delta\delta_{max}}{[S]_0}\left(\frac{1}{2}\left([R]_0+[S]_0+\frac{1}{K_a}\right) - \sqrt{\frac{1}{4}\left([R]_0+[S]_0+\frac{1}{K_a}\right)^2 - [R]_0[S]_0}\right) \tag{3}$$

In the titration experiments, the total substrate concentration [S]$_0$ was kept constant, whereas the total receptor concentration [R]$_0$ was varied. This was achieved by dissolving a defined amount of receptor R in 0.6 mL of a solution containing the substrate concentration [S]$_0$. $\Delta\delta$ was determined from the chemical shift of the pure substrate and the chemical shift of the substrate measured in the ^{1}H NMR spectrum (500 MHz, 25 °C) of this mixture. Successive addition of further solution containing [S]$_0$ leads to a dilution of the concentration [R]$_0$ in the mixture, while [S]$_0$ is kept constant. Measurement of the chemical shift of the substrate as a function of the concentration [R]$_0$ afforded the data pairs $\Delta\delta$ and [R]$_0$. Fitting of these data to the 1:1 binding isotherm by iterative methods[46] delivered the parameters K_a and $\Delta\delta_{max}$.

In the case of substrates having more than one kind of nonequivalent protons, the determination of the association constants K_a sometimes leads to different values of K_a. This may result from increasing errors caused by decreasing $\Delta\delta_{max}$ values. To minimize such errors the association constants K_a were determined for that proton of the substrate S displaying the largest value for $\Delta\delta_{max}$. The $\Delta\delta_{max}$ values of the other kind of substrate protons were calculated by use of Equation (5). Equation (5) was derived from the relationship between [RS] and the observed $\Delta\delta$ and $\Delta\delta_{max}$ of each kind of guest protons shown in Equation (4).

$$[RS] = [S]_0\frac{\Delta\delta_1}{\Delta\delta_{1,max}} = [S]_0\frac{\Delta\delta_2}{\Delta\delta_{2,max}} = [S]_0\frac{\Delta\delta_n}{\Delta\delta_{n,max}} \tag{4}$$

$$\Delta\delta_{n,max} = \delta_n\frac{\Delta\delta_1}{\Delta\delta_{1,max}} \tag{5}$$

The corresponding maximum complexation-induced shifts $\Delta\delta_{R,max}$ of the protons of the receptor R = **2b** were not determined due to its concentration-dependent chemical shifts. The observed shifts for all protons of **2b** in the absence of any substrate in the concentration range of 2.1×10^{-3} to 3.3×10^{-5} M in CDCl$_3$ is documented in the Supporting Information: Table S1.

Determination of the activation parameters $\Delta H^{\ddagger}$, $\Delta S^{\ddagger}$, and $\Delta G^{\ddagger}$ by line-shape analysis: The exchange frequency k of the investigated process was determined by simulation of the corresponding ^{1}H NMR spectra with the computer program WINDYNA.[47] The activation parameters are derived by utilizing the temperature dependence of the frequency k. The Arrhenius correlation is shown in Equation (6)

$$k = A\exp\left(-\frac{E_a}{RT}\right) \tag{6}$$

where k is the exchange frequency, A the preexponential factor, R the general gas constant, E_a the activation energy, and T the temperature.

The logarithmic form of the Arrhenius correlation is shown in Equation (7).

$$\ln k = \ln A - \frac{E_a}{R}\frac{1}{T} \tag{7}$$

The exchange frequencies k are determined iteratively at different temperatures. By the use of Equation (7) $\ln k$ is plotted against T^{-1}, and a linear regression analysis is performed. From this analysis the preexponential factor A results from the axis intercept and the activation energy E_a from the slope. From this data the activation parameters are finally calculated by the use of Equations (8)–(10)

$$\Delta S^{\ddagger} = R\left(\ln A - \ln\left(\frac{k_B T}{h}\right) - 1\right) \tag{8}$$

$$\Delta H^{\pm} = E_a - RT \tag{9}$$

$$\Delta G^{\pm} = \Delta H^{\pm} - T\Delta S^{\pm} \tag{10}$$

where A is the preexponential factor, E_a the activation energy, T the temperature, R the general gas constant ($1.987\,\mathrm{cal\,mol^{-1}\,K^{-1}}$), k_B the Boltzmann constant ($3.302 \times 10^{-24}\,\mathrm{cal\,mol^{-1}}$), and h the Planck constant ($1.584 \times 10^{-34}\,\mathrm{cal\,s}$).

Acknowledgement

[1] J. M. Lehn, *Supramolecular Chemistry—Concepts and Perspectives*, VCH, Weinheim, **1995**.

[2] H.-J. Schneider, A. Yatsimirsky, *Principles and Methods in Supramolecular Chemistry*, Wiley-VCH, Weinheim, **2000**.

[3] J. L. Atwood, J. W. Steed, *Supramolecular Chemistry*, Wiley-VCH, Weinheim, **2000**.

[4] M. Pons, O. Millet, *Prog. Nucl. Mag. Res. Spec.* **2001**, *38*, 267–324.

[5] D. J. Cram, *Abstr. Pap. Am. Chem. Soc.* **1997**, *213*, 389-ORGN.

[6] D. J. Cram, R. C. Helgeson, C. B. Knobler, E. F. Maverick, *Tetrahedron Lett.* **2000**, *41*, 9465–9470.

[7] K. N. Houk, K. Nakamura, C. M. Sheu, A. E. Keating, *Science* **1996**, *273*, 627–629.

[8] K. Nakamura, C. M. Sheu, A. E. Keating, K. N. Houk, J. C. Sherman, R. G. Chapman, W. L. Jorgensen, *J. Am. Chem. Soc.* **1997**, *119*, 4321–4322.

[9] D. B. Amabilino, P. R. Ashton, A. S. Reder, N. Spencer, J. F. Stoddart, *Angew. Chem.* **1994**, *106*, 450–458; *Angew. Chem. Int. Ed. Engl.* **1994**, *33*, 433–437.

[10] D. Pasini, F. M. Raymo, J. F. Stoddart, *Gazz. Chim. Ital.* **1995**, *125*, 431–443.

[11] S. A. Nepogodiev, J. F. Stoddart, *Chem. Rev.* **1998**, *98*, 1959–1976.

[12] M. Horn, J. Ihringer, P. T. Glink, J. F. Stoddart, *Chem. Eur. J.* **2003**, *9*, 4046–4054.

[13] S. J. Rowan, S. J. Cantrill, G. R. L. Cousins, J. K. M. Sanders, J. F. Stoddart, *Angew. Chem.* **2002**, *114*, 938–993; *Angew. Chem. Int. Ed.* **2002**, *41*, 898–952.

[14] T. Felder, C. A. Schalley, *Angew. Chem.* **2003**, *115*, 2360–2363; *Angew. Chem. Int. Ed.* **2003**, *42*, 2258–2260.

[15] V. Balzani, M. Venturi, A. Credi, *Molecular Devices and Machines—A Journey into the Nanoworld*, Wiley-VCH, Weinheim **2003**.

[16] E. P. Kyba, R. C. Helgeson, K. Madan, G. W. Gokel, T. L. Tarnowski, S. S. Moore, D. J. Cram, *J. Am. Chem. Soc.* **1977**, *99*, 2564–2571.

[17] L. J. Prins, D. N. Reinhoudt, P. Timmerman, *Angew. Chem.* **2001**, *113*, 2446–2492; *Angew. Chem. Int. Ed.* **2001**, *40*, 2383–2426.

[18] E. A. Meyer, R. K. Castellano, F. Diederich, *Angew. Chem.* **2003**, *115*, 1244–1287; *Angew. Chem. Int. Ed.* **2003**, *42*, 1210–1250.

[19] K. N. Houk, A. G. Leach, S. P. Kim, X. Y. Zhang, *Angew. Chem.* **2003**, *115*, 5020–5046; *Angew. Chem. Int. Ed.* **2003**, *42*, 4872–4897.

[20] A. R. Williams, B. H. Northrop, K. N. Houk, L. F. Stoddart, D. J. Williams, *Chem. Eur. J.* **2004**, *10*, 5406–5421.

[21] J. Rebek, *Acc. Chem. Res.* **1999**, *32*, 278–286.

[22] F. Hof, S. L. Craig, C. Nuckolls, J. Rebek, *Angew. Chem.* **2002**, *114*, 1556–1578; *Angew. Chem. Int. Ed.* **2002**, *41*, 1488–1508.

[23] S. V. Kolotuchin, S. C. Zimmerman, *J. Am. Chem. Soc.* **1998**, *120*, 9092–9093.

[24] R. K. Castellano, J. Rebek, *J. Am. Chem. Soc.* **1998**, *120*, 3657–3663.

[25] J. M. Lehn, *Proc. Natl. Acad. Sci. U.S.A.* **2002**, *99*, 4763–4768.

[26] F.-G. Klärner, J. Benkhoff, R. Boese, U. Burkert, M. Kamieth, U. Naatz, *Angew. Chem.* **1996**, *108*, 1195–1198; *Angew. Chem. Int. Ed. Engl.* **1996**, *35*, 1130–1133.

[27] F.-G. Klärner, U. Burkert, M. Kamieth, R. Boese, J. Benet-Buchholz, *Chem. Eur. J.* **1999**, *5*, 1700–1707.

[28] M. Kamieth, U. Burkert, P. S. Corbin, S. J. Dell, S. C. Zimmerman, F.-G. Klärner, *Eur. J. Org. Chem.* **1999**, 2741–2749.

[29] F.-G. Klärner, U. Burkert, M. Kamieth, R. Boese, *J. Phys. Org. Chem.* **2000**, *13*, 604–611.

[30] F.-G. Klärner, M. Lobert, U. Naatz, H. Bandmann, R. Boese, *Chem. Eur. J.* **2003**, *9*, 5036–5047.

[31] F.-G. Klärner, B. Kahlert, *Acc. Chem. Res.* **2003**, *36*, 919–932.

[32] M. Kamieth, F.-G. Klärner, F. Diederich, *Angew. Chem.* **1998**, *110*, 3497–3500; *Angew. Chem. Int. Ed.* **1998**, *37*, 3303–3306.

[33] F.-G. Klärner, J. Panitzky, D. Preda, L. T. Scott, *J. Mol. Model.* **2000**, *6*, 318–327.

[34] T. A. Halgren, *J. Comput. Chem.* **1996**, *17*, 490–519.

[35] SPARTAN 02, Wavefunction, Inc., 18401 Von Karman Avenue, Suite 370, Irvine, CA 92715.

[36] F. Marchioni, A. Juris, M. Lobert, U. P. Seelbach, B. Kahlert, F. G. Klarner, *New J. Chem.* **2005**, *29*, 780–784.

[37] The experimental determination of the activation parameters ΔH and ΔS by temperature-dependent NMR measurements is inaccurate due to the error-prone temperature determination at the probe and precise determination of the line broadening (T. M. Wang, J. S. Bradshaw, R. M. Izatt, *J. Heterocycl. Chem.* **1994**, *31*, 1097–1114).

[38] In the case of complex **3@1b** the rotation around the C_6 axis is blocked by the cyano groups, which are sterically too bulky to move through the tweezer cavity. In the case of complex **3@2a** the activation barrier for the rotation around the C_6 axis was calculated to be at least $20\,\mathrm{kcal\,mol^{-1}}$.

[39] The experimental ΔG values were determined in different solvents (association: CDCl$_3$, dissociation: [D$_8$]toluene) but it was shown that this influence (ΔG maximal $0.3\,\mathrm{kcal\,mol^{-1}}$) is very low. Therefore the diagrams are significant.

[40] E. Klingsberg, *Synthesis* **1972**, 29ff.

[41] M. Hanack, R. Großhans, *Chem. Ber.* **1992**, *125*, 1243–1247.

[42] M. P. Cava, D. R. Napier, *J. Am. Chem. Soc.* **1957**, *79*, 1701.

[43] M. P. Cava, R. L. Shirley, *J. Am. Chem. Soc.* **1960**, *82*, 654–656.

[44] M. N. Paddon-Row, H. K. Patney, K. Harish, *Synthesis* **1986**, 328–330.

[45] The molecular electrostatic potential (MEP) in the center of the terminal benzene unit of the naphthalene sidewalls is calculated by AM1 to be MEP$= -20.9$ or $-29.7\,\mathrm{kcal\,mol^{-1}}$ on the concave face of clip **2b** and **2a**, respectively.

[46] Nonlinear regression analysis of Equation (3) was performed by the use of the program TableCurve 4.0, SPSS Science, analogous to the computer program HOSTEST by C. S. Wilcox, N. M. Glagovich, University of Pittsburg and the program Associate V1.6, B. Peterson, Ph.D. Dissertation, University of California at Los Angeles, **1994**.

[47] WINDYNA, v. 1.01, Bruker Daltonik GmbH, **1998**.